The Enantioselective Organocatalytic [1,2]-Rearrangement of Allylic Ammonium Ylides

Will C. Hartley,[1] Mark D. Greenhalgh,[1,2] Kevin Kasten,[1] Taisiia Feoktistova,[3,‡] Henry B. Wise,[3,‡] Jacqueline M. Laddusaw,[3,‡] Aileen B. Frost,[1] Sean Ng,[4] Alexandra M. Z. Slawin,[1] Bela E. Bode,[1] Paul Ha-Yeon Cheong,[3*] Andrew D. Smith[1*]

[1]EaStCHEM, School of Chemistry, University of St Andrews, North Haugh, St Andrews, KY16 9ST, UK

[2]Department of Chemistry, University of Warwick, CV4 7AL, UK

[3]Department of Chemistry, Oregon State University, 153 Gilbert Hall, Corvallis, OR 97331, USA

[4]Syngenta, Jealott's Hill International Research Centre, Bracknell, Berkshire, RG42 6EY, UK

*e-mail: ads10@st-andrews.ac.uk; cheongh@oregonstate.edu

Abstract:

The [1,2]-rearrangement of allylic ammonium ylides is traditionally observed as a competitive minor pathway alongside the thermally allowed [2,3]-sigmatropic rearrangement. The challenges associated with developing a catalytic enantioselective variant are amplified as concerted [1,2]-rearrangements are forbidden, with these processes proposed to proceed through homolytic C-N bond fission of the ylide, followed by stereoselective radical-radical recombination. Herein a Lewis basic chiral isothiourea facilitates catalytic [1,2]-rearrangement of prochiral aryl ester ammonium salts to generate unnatural α-amino acid derivatives with unprecedented levels of enantiocontrol (up to 97:3 er) and up to total selectivity over the thermally allowed [2,3]-rearrangement. Key factors in favouring the [1,2]-rearrangement include exploitation of (i) disubstituted terminal allylic substituents, (ii) cyclic N-substituted ammonium salts and (iii) elevated reaction temperatures. Mechanistic studies involving ^{13}C-labelling and crossover reactions, combined with radical trapping experiments and observed changes in product enantioselectivity are consistent with a radical solvent cage effect, with maximum product enantioselectivity observed with promotion of "in-cage" radical-radical recombination. Computational analysis indicates that the distribution between [1,2]- and [2,3]-rearrangement products arises predominantly from C-N bond homolysis of an intermediate ammonium ylide, followed by recombination of the α-amino radical at either the primary or tertiary site of an intermediate allylic radical. Electrostatic interactions involving the bromide counterion and the rearrangement transition states control the facial selectivity of the [1,2]- and [2,3]-rearrangements, while the difficulty of forming a bond in the more sterically hindered tertiary position of the allylic substituent disfavors the formation of the [2,3]-product. These results will impact further investigations and understanding into enantioselective radical-radical reactions.

1

The dichotomy between competitive [1,2]- and [2,3]-rearrangements of onium ylides has been of long-standing interest to the synthetic community. Stevens reported the first [1,2]-rearrangement of a benzylic ammonium ylide in 1928,[1] with the mechanism of this rearrangement thoroughly investigated and of widespread interest as concerted [1,2]-rearrangeements are forbidden by the Woodward-Hoffman rules. Wittig[2] and Hauser[3] demonstrated that [1,2]-rearrangement proceeds with retention of configuration at the migrating carbon.[4] The most widely-accepted mechanistic explanation comes from detailed experiments by Ollis,[5–7] which indicate homolytic C−N bond cleavage of the ammonium ylide generates a geminate radical pair that undergoes preferential "intramolecular" radical-radical recombination (Figure 1a). Experiments using an enantiopure benzylic ammonium salt **1** showed up to 99% enantiospecificity in viscous solvents, leading to the suggestion that radical-radical recombination takes place within the solvent cage at a faster rate (estimated at $>10^{11}$ s^{-1})[7] than molecular rotation or cage escape/diffusion of either of the radical partners (Figure 1a). The [1,2]-rearrangement of benzylic ammonium ylides has been most-widely studied as the competing [2,3]-rearrangement process (Sommelet-Hauser) is significantly disfavoured due to the requirement for transient dearomatisation. In contrast, allylic ammonium ylides typically give product mixtures that are ascribed to competitive [1,2]- and [2,3]-rearrangement, with the [1,2]-product usually being a minor reaction pathway. A range of factors influence the ratio of [1,2]- and [2,3]-products; strong bases and aprotic solvents,[8] higher reaction temperatures,[5,6,9] and the use of sterically-congested and unstabilised ylides typically lead to a greater proportion of [1,2]-rearrangement.[5,6,10] The current state-of-the-art understanding of these processes has been provided by Singleton and co-workers, with [1,2]- and [2,3]-rearrangement product mixtures shown to arise from a common transition state in which homolytic C−N bond cleavage is promoted by a loose [2,3]-transition state, leading to 20% of the [1,2]-product at 90 ˚C (Figure 1b).[8,9]

Current asymmetric approaches to [1,2]-rearrangements of ammonium ylides are limited, and generally rely upon either stoichiometric chiral auxiliaries[11,12] or *stereospecific* rearrangements through N-to-C chirality transfer.[13-15] *Catalytic enantioselective* approaches are rare, with the difficulty in controlling radical-radical recombinations leading to this being a recognised challenge in enantioselective synthesis. The current state-of-the-art is represented by the work of Arnold and coworkers who recently established a biocatalytic [1,2]-Stevens type ring expansion of aziridines.[16] Single examples of a phosphite-catalysed enantioselective [1,2]-rearrangement of an N-benzylic isoquinoline derivative (94:6 er),[17] and a copper-catalysed enantioselective [1,2]-rearrangement of an allylic sulfonium ylide (69:31 er) have been demonstrated.[18] During the finalisation of this work, enantioselective variants involving ring-expansion of conformationally restricted azetidine-derived allylic ammonium ylides that proceed through a stepwise intramolecular ion-pair pathway have been reported.[19, 20]

In previous work, we developed the isothiourea-catalysed enantioselective [2,3]-rearrangement of allylic ammonium ylides (Figure 1c).[21] Experimental and computational studies led to the proposal of a highly stereodefined transition state **TS-I**, in which stereocontrol is governed by: (i) the (*Z*)-

2

configuration of the enolate-like yllide; (ii) a 1,5-O•••S chalcogen interaction that locks the conformation of the acylated catalyst; (iii) the phenyl substituent of the catalyst promoting facial-selectivity for rearrangement; and (iv) a π•••isothiouronium interaction between the cinnamyl Ph substituent and the acylated catalyst.[22] Building upon Singleton's proposition of common [1,2]- and [2,3]-transition states, we rationalised that access to pre-organised [2,3]-transition state **TS-I** could be exploited to develop a catalytic enantioselective [1,2]-rearrangement through incorporating steric hindrance at the terminal allylic substituent while exploiting solvent polarity and increasing reaction temperature (Figure 1c, grey box). Herein is described a catalytic protocol using a commercially available isothiourea catalyst, tetramisole hydrochloride, to provide unnatural α-amino acid derivatives in excellent enantioselectivity. Detailed mechanistic studies indicate that maximising pseudo-intramolecular "in-cage" radical-radical recombination is a requirement to generate the [1,2]-product with high enantiocontrol. Computational analysis supports the hypothesis of common [1,2]- and [2,3]-transition states and indicates that the [1,2]-product is formed via preferential C-N bond homolysis of an ylide intermediate, followed by stereoselective recombination of an allylic radical with a catalyst-bound captodative radical.
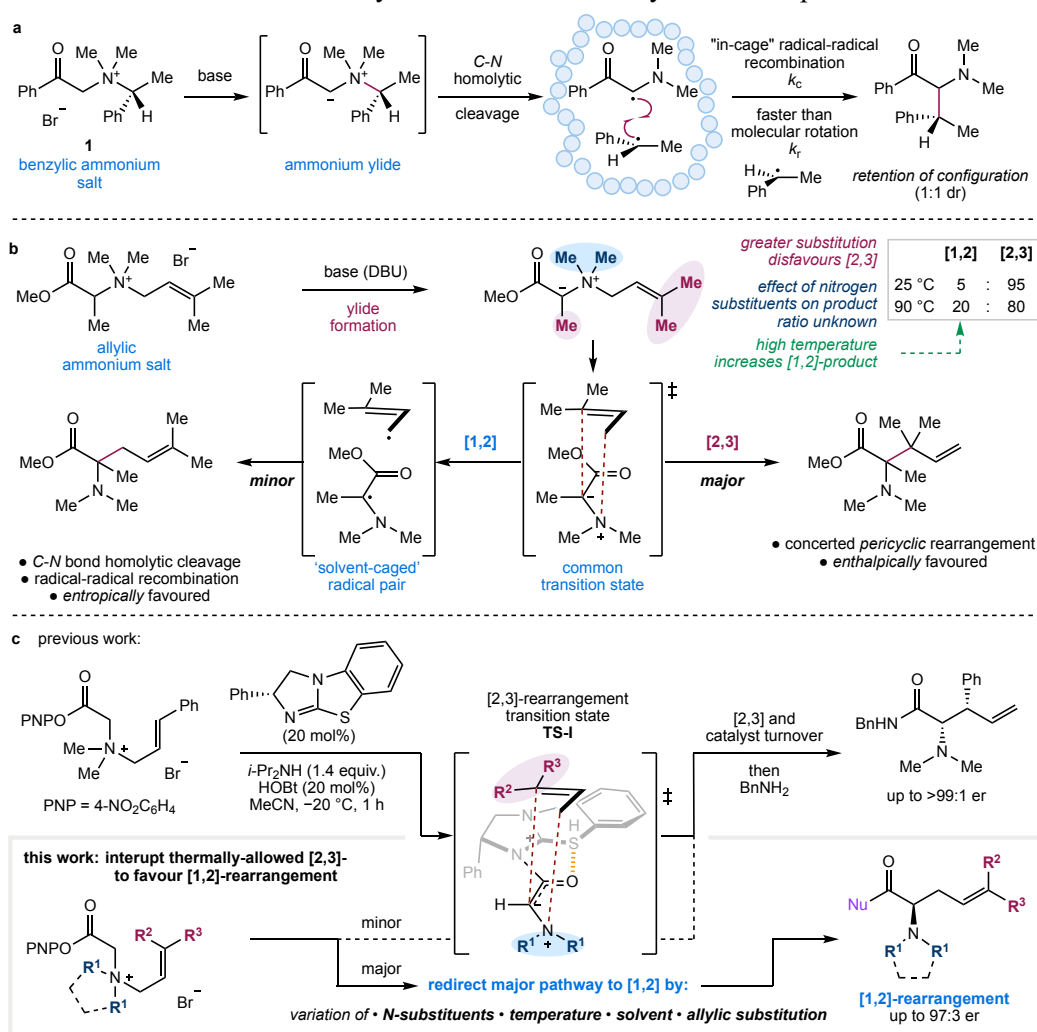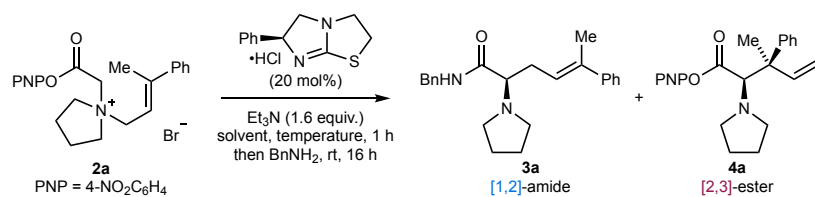
Figure 1: **a** [1,2]-Rearrangement of benzylic ammonium ylide, first reported by Stevens *et al.* in 1928. **b** Competitive [1,2]- and [2,3]-rearrangement of allylic ammonium ylides. **c** Previous studies and this work: Isothiourea-catalysed enantioselective [2,3]- and [1,2]-rearrangements of allylic ammonium ylides.

Results and Discussion

Optimisation of the [1,2]-rearrangement was conducted using ammonium salt **2a**, bearing a terminal disubstituted allyl substituent to disfavour the [2,3]-rearrangement product (Table 1). MeCN was chosen as the reaction solvent due to its high polarity and compatibility with the substrate and catalyst. Using tetramisole·HCl (TM·HCl) as the Lewis base catalyst at 30 °C resulted in high conversion within 1 h to a 67:33 mixture of [1,2]- and [2,3]-rearrangement products **3a** and **4a** (Table 1, entry 1). Selective amidation of the [1,2]-rearrangement product ester with benzylamine simplifed chromatographic separation and gave amide **3a** in 57% and 93:7 er, validating the feasibility of a catalytic enantioselective protocol. Increasing the reaction temperature to 40 °C resulted in improved [1,2]-rearrangement selectivity (80:20) without significant impact on enantioselectivity (entry 2, 70%, 92:8 er). Sequentially increasing the reaction temperature to 50 °C and 60 °C resulted in further improvements in [1,2]-rearrangement product selectivity, but lower enantioselectivity (entries 3 and 4). A reaction temperature of 50 °C was considered an optimal compromise, providing the [1,2]-rearrangement product **3a** in 72% isolated yield and 91:9 er. Control reactions confirmed that [2,3]-rearrangement product ester **4a** does not isomerise to the [1,2]-rearrangement product under the standard reaction conditions, indicating the origin of this trend in product selectivity is not thermodynamic in nature. *In situ* reaction monitoring revealed a consistent ratio of [1,2]- to [2,3]-reaction products throughout the course of the reaction, again consistent with no interchange of [1,2]- and [2,3]-intermediates or products under the reaction conditions (see SI section F for details). The use of alternative solvents of varying dielectric constant and viscosity were also investigated. Dichloromethane as a solvent gave significantly lower [1,2]:[2,3]-rearrangement selectivity (entry 5), while dimethylacetamide (DMA) and ethylene carbonate (EC) provided good [1,2]:[2,3]-rearrangement selectivity, and marginally improved enantioselectivity relative to MeCN (entries 6 and 7). However, reactions in DMA led to significantly lower product yield (36%), whilst EC complicated product isolation due to competitive reaction with benzylamine to give a carbamate side product. The absolute configuration of (*R,E*)-**3a** was proven by crystallographic analysis, consistent with isomerisation of the allylic fragment not being observed in the generation of the [1,2]-product. The relative configuration of the [2,3]-rearrangement product **4a** was assigned by comparison to X-ray analysis of analogue **4j** (see **SI** section E).
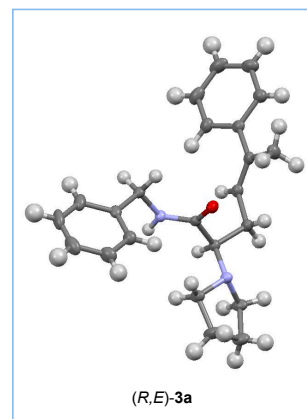
4

Table 1: Reaction optimisation. Yields and [1,2]:[2,3] rearrangement product ratios calculated by ^{1}H NMR analysis of the crude reaction product using 1,4-dinitrobenzene as internal standard; numbers in parentheses correspond to isolated yields. DMA = dimethylacetamide. EC = ethylene carbonate. [a] 80:20 dr; major diastereoisomer obtained in 78:22 er. [b] Sealed tube.

entry	solvent	temperature	yield [1,2] [%]	er [1,2]	yield [2,3] [%]	[1,2]:[2,3]
1	MeCN	30 °C	57	93:7	29	67 : 33
2	MeCN	40 °C	70	92:8	17	80 : 20
3	**MeCN**	**50 °C**	**75 (72)**	**91:9**	**14 (11)[a]**	**84 : 16**
4	MeCN	60 °C	76	84:16	12	86 : 14
5	CH$_2$Cl$_2$[b]	50 °C	32	89:11	17	67 : 33
6	DMA	50 °C	36	93:7	7	84 : 16
7	EC	50 °C	68	94:6	21	75 : 25

With optimised conditions developed, the scope of the reaction was investigated. The effect of structural variation within the allylic substituents was probed (Figure 2a). Sequentially changing the R^2 substituent from methyl **3a** through ethyl **3b** and iso-propyl **3c** increased the ratio of [1,2]:[2,3]-rearrangement products from 84:16 to 90:10 to 93:7 (Figure 2a), alongside a small reduction in enantioselectivity. Both fluorenyl and diphenyl substitution gave exclusive [1,2]-rearrangement products **3d** and **3e** in 83:17 and 77:23 er, respectively. *In situ* reaction monitoring of the rearrangement to give **3e** showed exclusive formation of the [1,2]-reaction product throughout the course of the reaction, again consistent with no interchange of [1,2]- and [2,3]-intermediates or products under the reaction conditions. The sequential increase in [1,2]-selectivity observed across this series is consistent with a combination of both increasing steric hindrance at the alkene terminus disfavouring [2,3]-rearrangement and increasing stability of an assumed allylic radical formed following C–N bond homolysis. Control experiments showed that prenyl substitution within the allylic fragment provided no rearrangement products, whilst consistent with previous work cinnamyl substitution gave exclusive [2,3]-rearrangement (95%, >95:5 dr, 93:7 er) (see SI for details). These experiments demonstrate the importance of (i) a terminal aryl substituent to promote reactivity; and (ii) terminal disubstitution to provide selectivity for the [1,2]-rearrangement.

Changing the nature of the R^1 N-substituents has a profound effect on the ratio of rearrangement products (Figure 2B). Variation of ring size showed that both piperidinyl and azepanyl derivatives provided preferential [1,2]-rearrangement, giving products **3f** and **3g** with 93:7 and 92:8 er, respectively. With acyclic *N,N*-dimethylamino substitution, [2,3]- or [1,2]-selectivity was dependent upon the nature of the terminal allylic substituents. Exclusive [1,2]-rearrangement was observed with diphenyl substitution (R^2, R^3=Ph) to give **3h** in 70:30 er. However when R^2=Me, the [2,3]-rearrangement product was preferred ([1,2]:[2,3] = 25:75), with the major diastereoisomer of the [2,3]-rearrangement product **4i** and the [1,2]-rearrangement product **3i** both isolable in high enantiopurity (90:10 er). Morpholinyl substitution resulted in highly-selective [2,3]-rearrangement ([1,2]:[2,3] =

5

17:83), and while the [1,2]-rearrangement product could not be isolated, the [2,3]-rearrangement product **4j** was obtained in 48% yield and 77:23 er (major diastereoisomer). The relative and absolute configuration within **4j** was confirmed by X-ray analysis (See SI section E for details).

Next, variation of the terminal aryl substituent R^3 was investigated (Figure 2C). Introduction of methyl and *tert*-butyl groups in the *para*-position gave the desired rearrangement products **3k** and **3l** in 58% and 61% yield, respectively, and 91:9 er in both cases. With a *para*-NO$_2$ electron-withdrawing group, the rearrangement was less efficient, leading to 47% of [1,2]-product **3m** in 84:16 er. *Para*-halogen substitution with fluorine, bromine and iodine gave the [1,2]-products **3n**–**3p** in good yield, with progressively greater preference for [1,2]-rearrangement, while enantioselectivity remained high (~90:10 er). *Ortho*- and *meta*-substitution was also well-tolerated, with **3q** and **3r** obtained in moderate yield but with high [1,2]-rearrangement selectivity. Finally, a range of nucleophiles can be used following the catalytic reaction to access different functional groups. Addition of sodium ethoxide gave ethyl ester **3s** in good yield and 91:9 er, while addition of pyrrolidine gave tertiary amide **3t** in excellent yield and 90:10 er. Pleasingly, addition of lithium aluminium hydride to the crude reaction product mixture after solvent exchange gave aminoalcohol **3u** in good yield with no erosion of enantiopurity. The reaction can also be carried out on gram-scale, with propargylic amide **3v** obtained in good yield and 88:12 er.
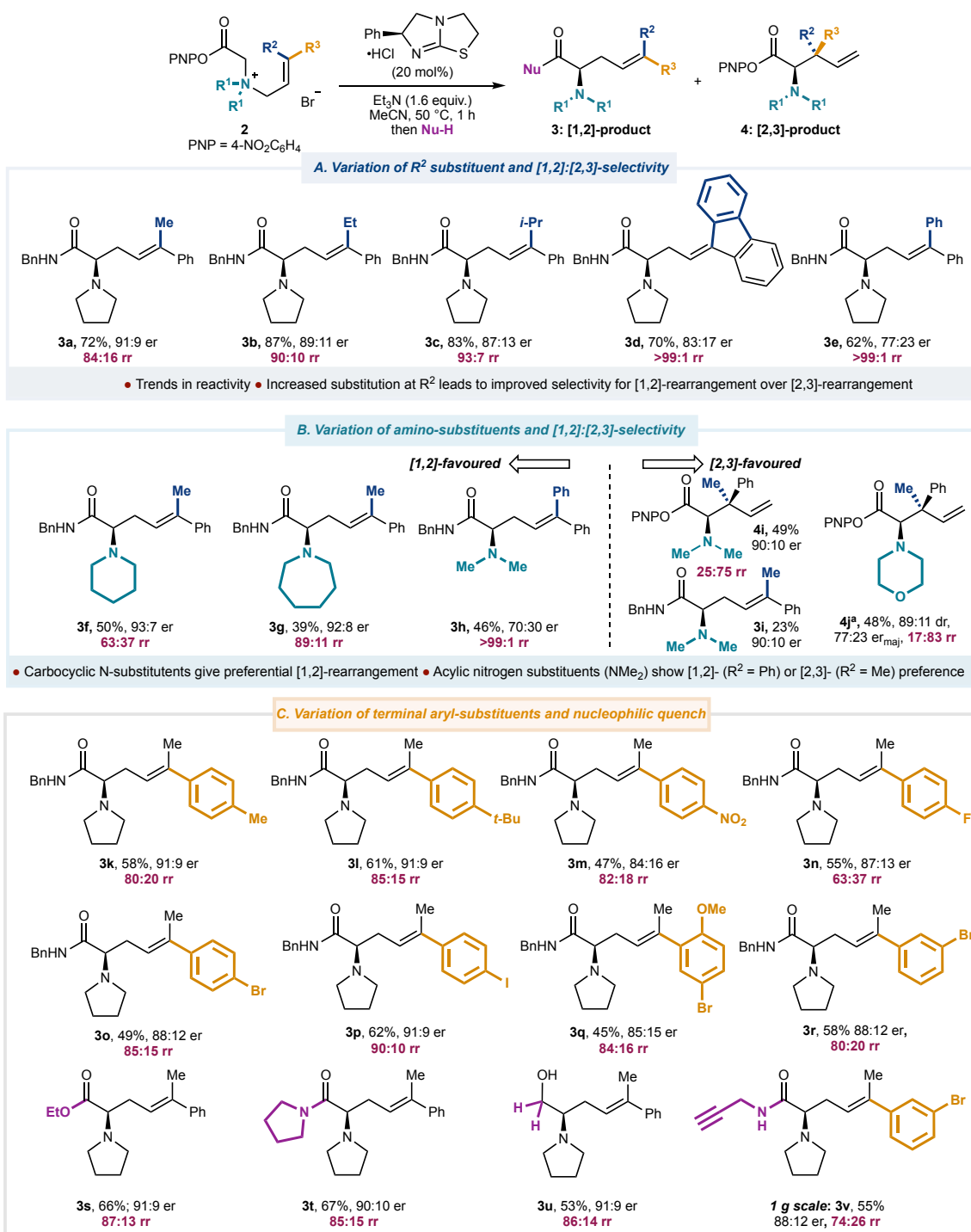
6

Figure 2: Scope of the reaction. Isolated yields given. [1,2]:[2,3] product ratio calculated by ^{1}H NMR analysis of the crude reaction product. [a] [1,2]-rearrangement product not isolated. [b] reaction carried out on 1 g scale. **a** Variation of R[2]. **b** Variation of R[1]. **c** Variation of R[3] and nucleophile added at the end of the reaction. rr = rearrangement product ratio ([1,2]:[2,3]).

Mechanistic investigations were then carried out to provide an in-depth understanding of the fundamental principles that underpin this catalytic enantioselective [1,2]-rearrangement. Crossover experiments were used to assess the intra- and intermolecular distribution of both the [1,2]- and [2,3]-rearrangement products. As the rearrangement product distributions are highly sensitive to structural variation, minimising the use of chemically differentiated substrates was deemed of paramount

7

importance for experimental design. For this purpose, a series of allylic ammonium salts containing a single ^{13}C-enriched isotopic label were prepared. Treatment of a 1:1 mixture of salts 2-[^{13}C$_1$]-**2a** and 2'-[^{13}C$_1$]-**2a** under the optimised conditions and analysis of the resultant isolated [1,2]-rearrangement product indicated significant (12%) crossover (Figure 3a, entry 1). Analogous treatment of a 1:1 mixture of salts 2-[^{13}C$_1$]-**2a** and 4'-[^{13}C$_1$]-**2a** indicated that the [2,3]-rearrangement product contained significantly reduced (2.6%) crossover (See SI Figure S12 for details). This is consistent with observations by Singleton who also observed increased crossover in [1,2]-products than [2,3]-products.[9] While Lehn and Kitching have shown that simple allylic and benzylic ammonium salts readily undergo salt exchange and metathesis,[23,24] control studies indicate that salt metathesis processes (that could potentially allow ammonium substituent exchange and therefore crossover within starting materials) are not observed in this system under typical reaction conditions (See SI Figure S10 for details). As a consequence, the observation of crossover products is taken as a measure of the intermolecularity of the [1,2]- and [2,3]-rearrangement processes. In the [1,2]-rearrangement case this is assumed to be representative of competition between "in-cage" radical-radical recombination (considered as "pseudo-intramolecular") or diffusion of the radicals followed by recombination (considered as "intermolecular"). A radical trap experiment using 1 equivalent of TEMPO did not fully inhibit the reaction, but gave the [1,2]-rearrangement product in a lower product yield (30%) with drastically reduced product intermolecularity (0.9%) and a substantial increase in enantiopurity (97:3 er). TEMPO adduct **5** was isolated in 8% yield, consistent with TEMPO trapping an allylic radical intermediate (Figure 3a). The use of a viscous and polar solvent,[25,26] ethylene carbonate, resulted in reduced intermolecularity (3.9%) with the [1,2]-rearrangement product again obtained with enhanced enantiopurity (94:6 er). Rearrangement of the corresponding ^{13}C-labelled diphenyl-substituted salts 2-[^{13}C$_1$]-**2e** and 2'-[^{13}C$_1$]-**2e** gave [1,2]-rearrangement product **3e** in 77:23 er with significant levels of intermolecularity (32%). Performed in the presence of TEMPO, this rearrangement proceeded with remarkably reduced intermolecularity (0.4%) and increased product enantioselectivity (86:14 er) as well as giving 11% of the TEMPO-adduct **6**. To further probe the consistent trend in higher product enantioselectivity with reduced intermolecularity, the [1,2]-rearrangement products arising from the ^{13}C-labelled diphenyl-substituted salts 2-[^{13}C$_1$]-**2e** and 2'-[^{13}C$_1$]-**2e** (both in the absence and presence of TEMPO) were further analysed through preparative separation of the product enantiomers (from samples of 71:29 er and 84:16 er respectively). In both instances, higher intermolecularity was observed in the (*S*)-enantiomer (50% intermolecularity without TEMPO, 2% with TEMPO) than the (*R*)-enantiomer (29% intermolecularity without TEMPO, 0.3% with TEMPO). Using this data, the enantioselectivitity of the inter- and pseudo-intramolecular processes can be calculated. In both the absence and presence of TEMPO, the pseudo-intramolecular process is highly enantioselective (calculated as 78:22 and 84:16 er, respectively), whilst the intermolecular process leads to significantly reduced product enantioselectivity giving close to racemic product (59:41 and 44:56 er, respectively).

8

These experiments are consistent with "in-cage" radical-radical recombination being essential for high enantioselectivity, with the addition of TEMPO increasing product enantioselectivity by efficiently trapping the diffused radicals to minimise the intermolecular reaction that proceeds with reduced enantioselectivity. A cyclopropyl-substituted allyl substrate **2w** was next prepared as a control to probe the rate of recombination within the radical cage (Figure 3b). Despite an assumed rate of ~10^8 s^{-1} for the ring opening of an intermediate cyclopropyl methyl radical, only the [1,2]-product **3w** was observed, consistent with the rate of radical recombination (previously estimated as >10^{11} s^{-1})[7] outcompeting ring-opening of the cyclopropyl fragment (Figure 3b).[27] The possibility of *in situ* identification of diffused radical intermediates was next sought. Given the significant 32% intermolecularity measured for the [1,2]-rearrangement of diphenyl substituted salt **2e**, this substrate was selected for EPR studies (Figure 3c). Initial attempts to directly detect radical intermediates proved unsuccessful, largely hampered by strong microwave absorption of the reaction solution. To overcome this, an alternative approach was undertaken through monitoring the consumption of TEMPO by EPR in two distinct rearrangement reactions. Firstly, the rearrangement of diphenyl-substituted salt **2e** (R = Ph), which proceeds with complete [1,2]-selectivity, and secondly the rearrangement of cinnamyl-substituted salt **2x** (R = H), which proceeds with complete [2,3]-selectivity. A flow set up was used so the reaction solution could be passed directly through the EPR spectrometer and allow *in situ* reaction monitoring. Applying 0.5 equivalents of TEMPO in each reaction resulted in ~0.1 equivalents being consumed during the [1,2]-rearrangement of **2e**, whereas the concentration of TEMPO remained constant during the [2,3]-rearrangement of **2x**. These results are consistent with direct trapping of the allylic radical as TEMPO adduct **6** during the [1,2]-rearrangement, whilst no analogous product, or consumption of TEMPO, was identified from the [2,3]-rearrangement of **2x**.

9

PNPO... 2-[$^{13}C_1$]-**2**

2'-[$^{13}C_1$]-**2**
PNP = 4-NO$_2$C$_6$H$_4$
● = ^{13}C label

TM·HCl (20 mol%)
Et$_3$N (1.6 equiv.)
MeCN, 50 °C, 1 h
then BnNH$_2$
(1.5 equiv.)
rt, 16 h

BnHN... 2-[$^{13}C_1$]-**3**
intramolecular [1,2]-products

BnHN... 2,3-[$^{13}C_2$]-**3**
intermolecular [1,2]-products

BnHN... 3-[$^{13}C_1$]-**3**

BnHN... **3**

5, R = Me
6, R = Ph

entry	R	deviation from standard conditions	yield [1,2] [%]	intermolecularity	er [1,2]	TEMPO-adduct
1	Me	-	72	11.8%	91:9	-
2	Me	TEMPO (1 equiv.)	30	0.9%	97:3	8%
3	Me	ethylene carbonate as solvent	69	3.9%	94:6	-
4	Ph	-	62	32.0%	77:23	-
5	Ph	TEMPO (1 equiv.)	46	0.4%	86:14	11%

3e
from entry 4
71:29 er (*R:S*)
32% intermolecularity

71% → preparative separation of enantiomers ← 29%

(*R*)-enantiomer
^{13}C NMR analysis:
29% intermolecularity

(*S*)-enantiomer
^{13}C NMR analysis:
50% intermolecularity

effective enantioselectivity:
intramolecular process: **78:22 er**
intermolecular process: **59:41 er**

3e
from entry 5 (TEMPO)
84:16 er (*R:S*)
0.5% intermolecularity

84% → preparative separation of enantiomers ← 16%

(*R*)-enantiomer
^{13}C NMR analysis:
0.3% intermolecularity

(*S*)-enantiomer
^{13}C NMR analysis:
2% intermolecularity

effective enantioselectivity:
intramolecular process: **84:16 er**
intermolecular process: **44:56 er**

b

2w 2:1 (*E:Z*)

(±)-**TM·HCl** (20 mol%)
Et$_3$N (1.6 equiv.)
MeCN, 50 °C, 1 h
then BnNH$_2$ (1.5 equiv.)
rt, 16 h

3w 4:1 (*E:Z*)
43%

no cyclopropyl ring-opening observed
⇓
recombination faster than ring-opening (10^8 s^{-1})

c

R = Ph
exclusive [1,2]
‣ [TEMPO] decreases during [1,2]-rearrangement reaction
‣ ~0.1 equiv. of TEMPO consumed

3e: [1,2]

2e: R = Ph
2x: R = H

EPR reaction monitoring in flow

conditions
TM·HCl (20 mol%)
Et$_3$N (1.6 equiv.)
TEMPO (0.5 equiv.)
MeCN (0.02 M), 50 °C

R = H
exclusive [2,3]
‣ [TEMPO] remains constant throughout [2,3]-rearrangement
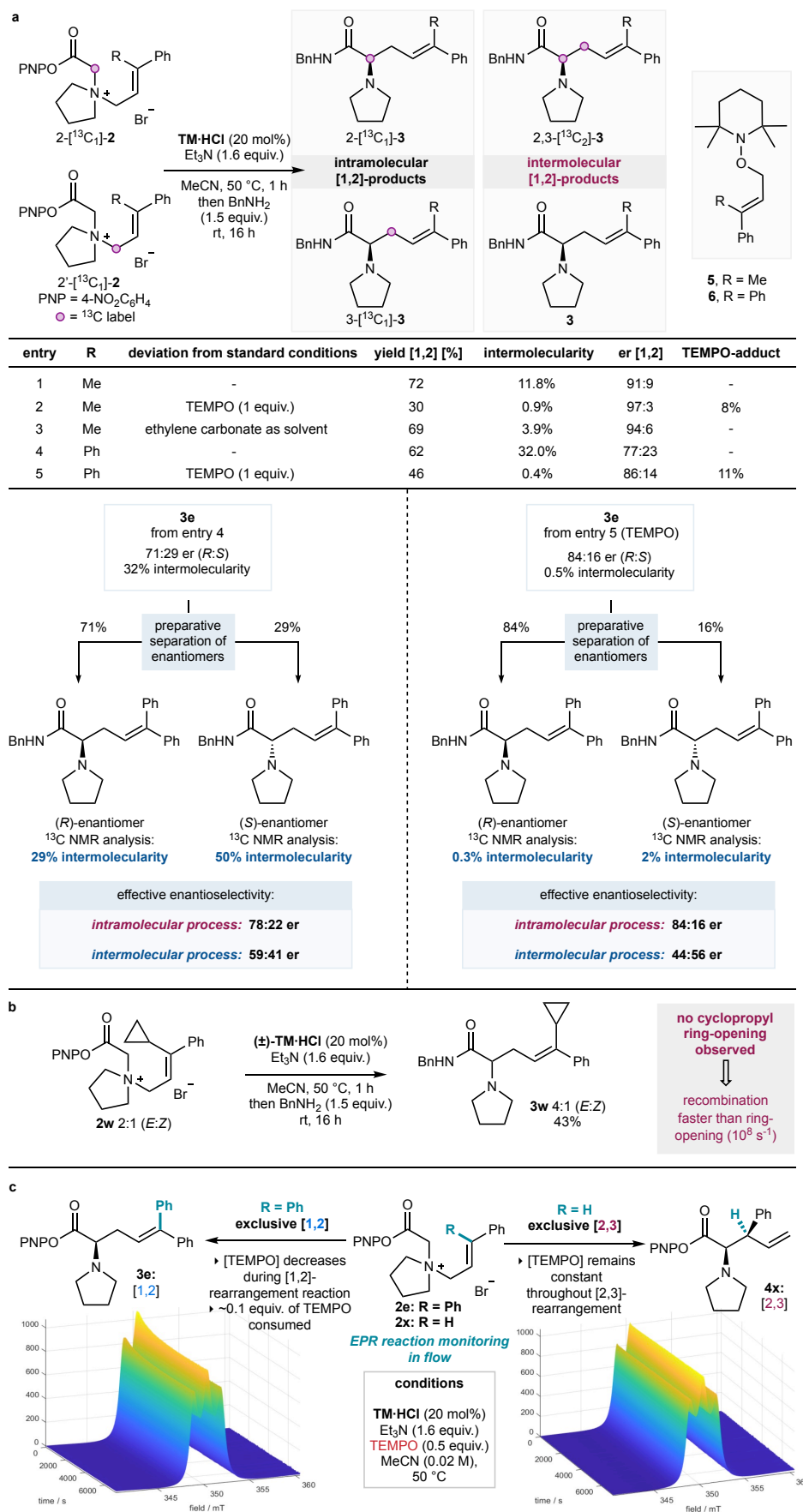
4x: [2,3]

Figure 3: **a** Crossover experiments to determine intermolecularity of [1,2]-rearrangement. Isolated yields given. Intermolecularity calculated through quantitative ^{13}C{^{1}H}-NMR analysis of purified [1,2]-rearrangement product, with

extended delay (d1 = 43 s) to allow full relaxation of active nuclei (see SI for full details). **b** Reaction of cyclopropyl containing substrate **2w**. **c** EPR spectroscopic monitoring of TEMPO concentration in the rearrangement of **2e** (left) and **2x** (right).

DFT was used to further investigate the mechanism and periselectivity of this reaction using tetramisole and allylic ammonium salt substrate **2a**, with UM06/6-31G*/PCM(acetonitrile) at 50 °C with Grimme's D3 empirical dispersion corrections as implemented in Gaussian16. The proposed catalytic cycle is shown in Figure 5. Notably, the inclusion and location of the bromide counterion that participates in multiple non-covalent stabilising C-H/N-CH•••Br⁻ interactions[28–37] within all structures on the catalytic cycle was critical for attaining relative transition state energies that reproduce the experimentally observed preferential formation of the [1,2]-rearrangement product. In addition, exploration of the rearrangement for all transition structures involving both facial approaches of the reactive allylic group for [1,2]- and [2,3]-processes was established, with the lowest energy structures used to construct the catalytic cycle (Figure 5).

Initial acylation of isothiourea catalyst tetramisole by the allylic ammonium salt **2a** liberates 4-nitrophenoxide to give an **acyl ammonium** complex ($\Delta G = -1.2$ kcal/mol). Deprotonation by 4-nitrophenoxide (**deprotonation-TS**, $\Delta G^{\ddagger} = 11.6$ kcal/mol) results in formation of the reactive **acyl ammonium ylide** at 8.1 kcal/mol, with onwards competitive reaction pathways feasible to generate the observed [1,2]- and [2,3]-products (See SI section H for full details). While the **acyl ammonium ylide** can undergo a **concerted-[2,3]** sigmatropic rearrangement process ($\Delta G^{\ddagger} = 18.9$ kcal/mol) to generate the **(R,R)**-[2,3]-intermediate ($\Delta G = -4.1$ kcal/mol), extensive efforts to find a concerted [1,2]-sigmatropic rearrangement from the **acyl ammonium ylide** failed to locate this transition state, consistent with this being a Woodward-Hoffman thermally forbidden process. Instead, homolytic C-N bond cleavage (**C–N Homolysis-TS**, $\Delta G^{\ddagger} = 17.3$ kcal/mol) is preferred to concerted rearrangement and generates a solvent caged **geminate radical pair** ($\Delta G = 10.6$ kcal/mol) consisting of the catalyst-bound captodative radical and a phenyl-conjugated allylic radical. Radical recombination preferentially occurs at the least hindered primary (C1) site of the allylic radical ([**1,2]-Radical Recombination TS**, $\Delta G^{\ddagger} = 11.9$ kcal/mol) to generate post-rearrangement acyl ammonium (**[1,2]-Intermediate**, $\Delta G = -14.4$ kcal/mol) as the favoured reaction pathway. Alternatively, recombination at the more hindered tertiary (C3) carbon of the allylic radical is feasible but higher in energy (**[2,3]-Radical Recombination TS**, $\Delta G^{\ddagger} = 13.0$ kcal/mol) leading to the **(R,S)**-[2,3]-intermediate ($\Delta G = -2.8$ kcal/mol). Subsequent turnover of catalyst-product complexes with 4-nitrophenoxide releases the observed ester products (**[1,2]-Product 3a** and diastereoisomeric **[2,3]-Products**) and regenerates the tetramisole isothiourea catalyst.
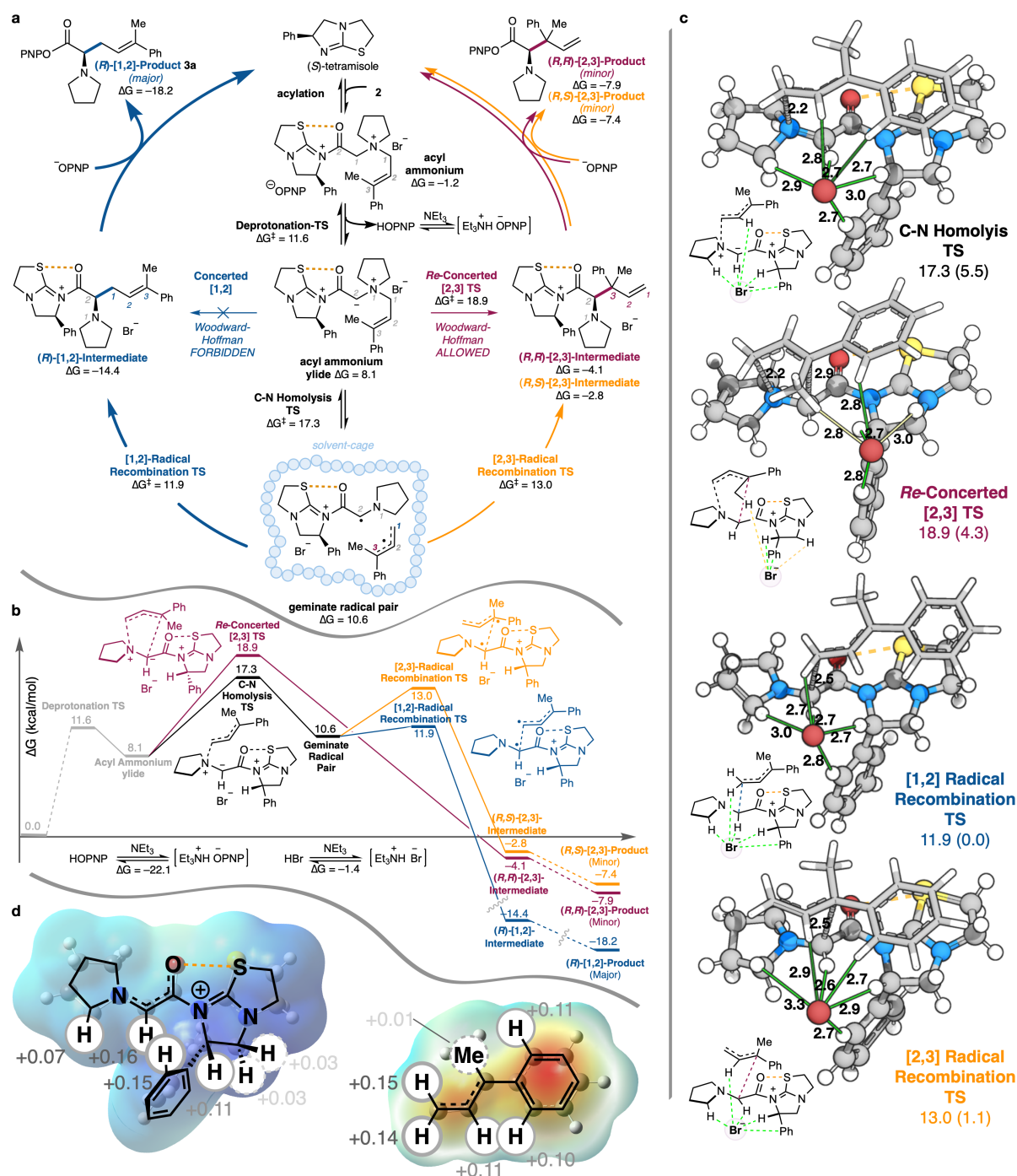
11

Figure 5: **a**. Proposed catalytic cycle and computed energies. [1,2]-product forming processes shown on left (blue), and the minor [2,3]-product forming processes shown on the right (red and orange). **b**. computed reaction progress profile. **c**. Computed transitions states (TS) for the C–N homolysis, concerted [2,3]-sigmatropic rearrangement, and radical recombination processes that lead to [1,2]- and [2,3]-products. Green and yellow lines denote strong and weak electrostatic interactions, respectively. **d**. Electrostatic potential maps and ChelpG charges of the acylated catalyst cation radical (left) and allyl radical (right).

There are four factors that govern the selectivities observed in this reaction (Figure 5):

1) **Planarity of the acylated isothiourea catalyst structures:** All structures involving the acylated isothiourea are planar due to an O•••S chalcogen bonding interaction (n_O to σ^*_{S-C}). This preorganization forces the recombination to preferentially occur *anti-* to the stereodirecting

catalyst phenyl substituent and explains the observed absolute configuration of the [1,2]-rearrangement product.

2) **Location of bromide counterion in [1,2]-rearrangement structures:** The location of the bromide counterion to allow maximum stabilising C-H/N-CH•••Br⁻ electrostatic interactions was critical to reproduce the experimentally observed preference for the [1,2]-rearrangement product. Atomic charge analyses using ChelpG (Figure 5D) of the proposed intermediate radicals reveal that (i) the catalyst-bound captodative radical carries substantial positive charge at C(2)H (+0.16), $^{+}$N-CH (+0.11) and $^{+}$N-CPh-H (+0.15) substituents; (ii) the substrate pyrrolidine N-CH bears more partial positive charge than the distal catalyst Csp^3-H (+0.07 vs +0.03 respectively) and (iii) the Csp^2-H at C(1) and C(2) of the allylic substituent bears more partial positive charge than the Csp^3-H of the C(3)-methyl substituent (+0.11–0.15 vs 0.01, respectively). The lowest energy [1,2]-rearrangement transition state structure (**[1,2]-Radical Recombination-TS**) maintains preferential bromide co-ordination proximal to the catalyst-bound captodative radical pyrrolidine N-CH, with the allylic radical in a conformation that places the C(3)Me-substituent *syn* to the C=O of the acylated catalyst, maximising C-H/N-CH•••Br⁻ interactions (Figure 5c; green and yellow lines denote strong and weak electrostatic interactions, respectively). Alternative orientations of the allylic group lead to higher energy transition structures (See Supporting Information section H). The bromide position being proximal to the pyrrolidine N-CH is conserved in the **C-N homolysis TS** and the **[2,3]-Radical Recombination-TS** but it not observed in the **Re-Concerted-[2,3]-TS** where the C(3)Me-substituent is *anti* to the C=O of the acylated catalyst.

3) **Electrostatic interactions between the acyl ammonium ylide and the bromide counterion controls the stepwise vs concerted selectivity:** From the acyl ammonium ylide, a concerted [1,2]-transition structure could not be found consistent with this being a Woodward-Hoffman thermally forbidden transformation. The concerted [2,3]-rearrangement can in principle form the new C-C bond on either the *Re-* or the *Si-* face of the allylic fragment. [2,3]-Rearrangement involving the *Si-*face was not found as a stationary point on the potential energy surface – exhaustive efforts to locate this structure decomposed into the **C-N homolysis** transition structure, suggesting that C-N homolysis is the favoured process from this conformation. The only concerted [2,3]-rearrangement transition state found involves rearrangement through the *Re-*face of the allylic substituent (**Re-Concerted-[2,3]-TS**) which corresponds to the configuration of the major diastereoisomer of the [2,3]-product obtained experimentally (Figure 5c). In comparing these two pathways the **C-N homolysis** transition state is energetically preferred over the **Re-Concerted-[2,3]-TS** due to greater stabilizing electrostatic interactions with the bromide counterion.

13

4) **Steric Effects of the Allyl Substituents:** The regioselectivity between stepwise [1,2]- and stepwise [2,3]-recombination is determined by steric occlusion of C1 versus C3 of the allylic fragment. In the stepwise [1,2]-process (**[1,2]-Radical Recombination-TS**), the C-C bond forms at the primary C1 allylic carbon which experiences minimal steric repulsion. However, in the stepwise [2,3]-process the C-C bond forms at the more substituted tertiary C3 allylic carbon (**[2,3]-Radical Recombination-TS**). Distortion-interaction analysis reveals that indeed the **[2,3]-Radical Recombination-TS** is more distorted than the **[1,2]-Radical Recombination-TS**, consistent with the hypothesis that forming a bond to the tertiary carbon of the allylic fragment is energetically unfavourable (See Supporting Information section H). As expected, *Re*-**Concerted-[2,3]-TS**, which involves bond forming and breaking at both the primary and the tertiary carbons of the allylic group, experiences the greatest distortion, further explaining why the [1,2]- process is favored over both the concerted and the stepwise [2,3]-processes. Computational analysis of a model system in which the allylic group bears just a single phenyl substituent predicts a switch in selectivity to now favour the concerted [2,3]-process, in keeping with experimental results.

In summary, the first catalytic and enantioselective [1,2]-rearrangement of allylic ammonium ylides has been developed. The factors necessary for affecting [1,2]-rearrangement have been examined, with higher reaction temperature resulting in increased [1,2]:[2,3] rearrangement product ratio. Treatment of a range of terminally-substituted allylic ammonium salts with isothiourea catalyst tetramisole led to the [1,2]-rearrangement of allylic ammonium ylides, giving amino acid derivatives in up to 87% yield and 98:2 er. ^{13}C-Isotopic labeling in crossover and radical-trapping experiments have revealed an intriguing interplay between intermolecularity and enantioselectivity. Computational analysis indicates that C-N-bond homolysis from an acyl ammonium ylide intermediate, followed by regioselective radical recombination at the primary site of the intermediate allylic radical leads to the [1,2]-product. The [2,3]-product can be formed through either concerted [2,3]-sigmatropic rearrangement or radical recombination at the tertiary site of the allylic radical. The insights provided from this study, particularly regarding the relationship between intermolecularity and product enantioselectivity, will have important consequences for future investigations of solvent-caged enantioselective radical recombination reactions.

Data availability:

Data are available in the manuscript and supplementary materials. The research data supporting this publication can be accessed at https://doi.org/10.17630/589d51ac-993a-44cc-9247-8f295125ec46; data underpinning "The Enantioselective Organocatalytic [1,2]-Rearrangement of Allylic Ammonium Ylides". University of St Andrews Research Portal; PURE ID: 298800968. The supplementary

crystallographic data for this paper are available free of charge from the Cambridge Crystallographic Data Centre (CCDC) under accession numbers 2312496 and 2314746.

References

1. Stevens, T. S., Creighton, E. M., Gordon, A. B. & MacNicol, M. CCCCXXIII.—Degradation of quaternary ammonium salts. Part I. *J. Chem. Soc. Resumed* 3193–3197 (1928).

2. Wittig, G., Mangold, R. & Felletschin, G. Über die Stevens'sche und Sommelet'sche Umlagerung als Ylid-Reaktionen. *Justus Liebigs Ann. Chem.* **560**, 116–127 (1948).

3. Hauser, C. R. & Kantor, S. W. Rearrangement of benzyl ethers to carbinols by potassium amide. mechanism of isomerization of carbanions involving 1,2-shifts. *J. Am. Chem. Soc.* **73**, 1437–1441 (1951).

4. Woodward, R. B. & Hoffmann, R. –The conservation of orbital symmetry, *Angew. Chem. Int. Ed.* **8**, 781–853 (1969).

5. Jemison, R. W., Laird, T., Ollis, W. D. & Sutherland, I. O. Base catalysed rearrangements involving ylide intermediates. Part 1. The rearrangements of diallyl- and allylpropynyl-ammonium cations. *J. Chem. Soc. Perkin 1* 1436–1449 (1980).

6. Jemison, R. W., Laird, T., Ollis, W. D. & Sutherland, I. O. Base catalysed rearrangements involving ylide intermediates. Part 2. The Stevens [1,2] and [3,2] sigmatropic rearrangements of allylic ammonium ylides. *J. Chem. Soc. Perkin 1* 1450–1457 (1980).

7. Ollis, W. D., Rey, M. & Sutherland, I. O. Base catalysed rearrangements involving ylide intermediates. Part 15. The mechanism of the Stevens [1,2] rearrangement. *J. Chem. Soc. Perkin 1* 1009–1027 (1983).

8. Biswas, B. & Singleton, D. A. Controlling selectivity by controlling the path of trajectories. *J. Am. Chem. Soc.* **137**, 14244–14247 (2015).

9. Biswas, B., Collins, S. C. & Singleton, D. A. Dynamics and a unified understanding of competitive [2,3]- and [1,2]-sigmatropic rearrangements based on a study of ammonium ylides. *J. Am. Chem. Soc.* **136**, 3740–3743 (2014).

10. Heard, G. L. & Yates, B. F. Competing rearrangements of ammonium ylides: a quantum theoretical study. *J. Org. Chem*. **61**, 7276–7284 (1996).

11. Tayama, E. & Kimura, H. Asymmetric Sommelet–Hauser rearrangement of N-benzylic ammonium salts. *Angew. Chem. Int. Ed.* **46**, 8869–8871 (2007).

12. Tayama, E., Orihara, K. & Kimura, H. New synthetic routes to optically active α-quaternary α-aryl amino acid derivatives via the diastereoselective Stevens and Sommelet–Hauser rearrangements. *Org. Biomol. Chem.* **6**, 3673–3680 (2008).

13. Tuzina, P. & Somfai, P. Asymmetric Lewis acid mediated [1,2]-rearrangement of proline-derived ammonium ylides. *Org. Lett.* **11**, 919–921 (2009).

15

14.   Glaeske, K. W. & West, F. G. Chirality transfer from carbon to nitrogen to carbon via cyclic ammonium ylides. *Org. Lett.* **1**, 31–34 (1999).

15.   Tayama, E., Nanbara, S. & Nakai, T. Asymmetric [1,2] Stevens rearrangement of (*S*)-*N*-benzylic proline-derived ammonium salts under biphasic conditions. *Chem. Lett.* **35**, 478–479 (2006).

16.   Miller, D. C., Lal, R. G., Marchetti, L. A. & Arnold, F. H. Biocatalytic one-carbon ring expansion of aziridines to azetidines via a highly enantioselective [1,2]-Stevens rearrangement. *J. Am. Chem. Soc.* **144**, 11, 4739–4745 (2022).

17.   Rani, S., Dash, S. R., Bera, A., Alam, M. N., Vanka, K. & Maity, P. Phosphite mediated asymmetric N to C migration fort he synthesis of chiral heterocycles from primary amines. *Chem. Sci.* **12**, 8996–9003 (2021).

18.   Qu, J.-P., Xu, Z.-H., Zhou, J., Cao, C.-L., Sun, X.-L., Dai, L.-X. & Tang, Y. . Ligand-accelerated asymmetric [1,2]-Stevens rearrangment of sulfur ylides via decomposition of diazomalonates catalyzed by chiral bisoxazoline/copper complex. *Adv. Synth. Catal.* **351**, 308–312 (2009).

19.   Wang, K., Yang, L., Li, Y., Li, H., Liu, Z., Ning, L., Liu, X. & Feng, X. Asymmetric catalytic ring-expansion of 3-methyleneazetidines with α-diazo pyrazoamides towards proline-derivatives. *Angew. Chem. Int. Ed.* **62**, e202307249 (2023).

20.   De Oliveira Silva, A., Masand, S., Farah, A. O., Laddusaw, J., Urbina, K., Rodriguez-Alvarado, M., Lalancette, R., Cheong, P. H.-Y. & Brenner-Moyer, S. Organocatalytic enantioselective [1,2]-Stevens rearrangement of azetidinium salts. Preprint at 10.26434/chemrxiv-2023-zbzgm

21.   West, T. H., Daniels, D. S. B., Slawin, A. M. Z. & Smith, A. D. An isothiourea-catalyzed asymmetric [2,3]-rearrangement of allylic ammonium ylides. *J. Am. Chem. Soc.* **136**, 4476–4479 (2014).

22.   West, T. H., Walden, D. M., Taylor, J. E., Brueckner, A. C., Johnston, R. C., Cheong, P. H.-Y., Lloyd-Jones, G. C. & Smith, A. D. Catalytic enantioselective [2,3]-rearrangements of allylic ammonium ylides: a mechanistic and computational study. *J. Am. Chem. Soc.* **139**, 4366–4375 (2017).

23.   Kulcha, S. & Lehn, J.-M., Dynamic covalent chemistry of nucleophilic substitution component exchange of quaternary ammonium salts, *Chem. Asian. J.* **10**, 2484–2496 (2015).

24.   Walsh, M. P., Phelps, J. M., Lennon, M. E., Yufit, D. S. & Kitching, M. O., Enantioselective synthesis of ammonium salts, *Nature* 597, 70-76 (2021).

25.   Barry, J. T., Berg, D. J. & Tyler, D. R. Radical cage effects: comparison of solvent bulk viscosity and microviscosity in predicting the recombination efficiencies of radical cage pairs. *J. Am. Chem. Soc.* **138**, 9389–9392 (2016).

26.   Li, X., Ogihara, T., Abe, M., Nakamura, Y. & Yamago, S. The effect of viscosity on the diffusion and termination reaction of organic radical pairs. *Chem. Eur. J.* **25**, 9846–9850 (2019).

27.   Griller, D. & Ingold, K. U. Free-radical clocks. *Acc. Chem. Res.* **13**, 317–323 (1980).

16

28.   Reetz, M. T. New methods for the anionic polymerization of α-activated olefins. *Angew. Chem. Int. Ed.* **27**, 994–998 (1988).

29.   Reetz, M. T., Hütte, S. & Goddard, R. Tetrabutylammonium salts of CH-acidic carbonyl compounds: real carbanions or supramolecules? *J. Am. Chem. Soc.* **115**, 9339–9340 (1993).

30.   Reetz, M. T., Hütte, S. & Goddard, R. Synthetic and mechanistic aspects of anionic polymerization of (METH)acrylates initiated by metal-free salts of CH-acidic compounds. *J. Phys. Org. Chem.* **8**, 231–241 (1995).

31.   Reetz, M. T., Hütte, S. & Goddard, R. & Robyr, C. Synthesis, structure, and stereoselective reaction of a chiral hydroxy-stabilized metal-free enolate. *Chem. Eur. J.* **2**, 382–384 (1996).

32.   Reetz, M. T., Hütte, S. & Goddard, R. Supramolecular structure of the tetrabutylammonium salt of 2-phenylpropionitrile. *J. Prakt. Chem.* **341**, 297–301 (1999).

33.   Goddard, R., Herzog, H. M. & Reetz, M. T. Cation–anion CH⋯O− interactions in the metal-free phenolate, tetra-*N*-butylammonium phenol-phenolate. *Tetrahedron* **58**, 7847–7850 (2002).

34.   Albrecht, M., Müller, M., Mergel, O., Rissanen, K. & Valkonen, A. Anion–π interactions in salts with polyhalide anions: Trapping of I_4^{2-}. *Chem. Eur. J.* **16**, 5062–5069 (2010).

35.   Berkessel, A., Das, S., Pekel, D. & Neudörfl, J-M. Anion-binding catalysis by electron-deficient pyridinium cations. *Angew. Chem. Int. Ed.* **53**, 11660–11664 (2014).

36.   Shirakawa, S., Liu, S., Kaneko, S., Kumatabara, Y., Fukuda, A., Omagari, Y. & Maruoka, K. Tetraalkylammonium salts as hydrogen-bonding catalysts. *Angew. Chem. Int. Ed.* **54**, 15767 –15770 (2015).

37.   Matador, E., Iglesias-Sigüenza, J., Monge, D., Merino, P., Fernández, R. & Lassaletta, J. M. Enantio- and diastereoselective nucleophilic addition of *N-tert*-butylhydrazones to isoquinolinium ions through anion-binding catalysis. *Angew. Chem. Int. Ed.* **60**, 5096–5101 (2021).

Authors and Affiliations:

17

EaStCHEM, School of Chemistry, University of St Andrews, North Haugh, St Andrews, KY16 9ST, UK.

Will C. Hartley, Mark D. Greenhalgh, Kevin Kasten, Aileen B. Frost, Bela E. Bode, Alexandra M. Z. Slawin, Andrew D. Smith

Department of Chemistry, Oregon State University, 153 Gilbert Hall, Corvallis, OR 97331, USA

Taisiia Feoktistova, Henry B. Wise, Jacqueline M. Laddusaw, Paul Ha-Yeon Cheong

Department of Chemistry, University of Warwick, CV4 7AL, UK

Mark D. Greenhalgh

Syngenta, Jealott's Hill International Research Centre, Bracknell, Berkshire, RG42 6EY, UK

Sean Ng

Author Contributions: A.D.S. conceived the project; W.C.H., M.D.G., K.K. and A.D.S. designed the synthetic experiments; W.C.H., A.B.F., M.D.G. and K.K. carried out all synthetic experimental studies and analysed the reactions. W.C.H. and B.E.B. carried out EPR spectroscopy measurements. A.M.Z.S. carried out single crystal X-ray analysis. T.F. carried out the initial computational studies, H.B.W. carried out theoretical hypotheses and analyses, and J.M.L. completed the computational analyses for publication (all equal contributions) in consultation with P.H-Y.C. W.C.H., M.D.G., K.K., P.H.-Y.C and A.D.S. wrote the manuscript. M.D.G., P.H-Y.C and A.D.S. supervised and directed the evolution of the project. Correspondence regarding computation should be addressed to P.H-Y.C. all other correspondence should be addressed to A.D.S.

Corresponding Authors:

Correspondence to A.D.S. (ads10@st-andrews.ac.uk) and P.H.-Y.C. (cheongh@oregonstate.edu).

Ethics Declaration:

Competing interests:

The authors declare no competing interests.

18

Graphical Abstract

allylic ammonium salts

(PNP = 4-NO$_2$C$_6$H$_4$)

organocatalysis

Catalytic Enantioselective [1,2]-Rearrangement

α-amino acid derivatives

up to **97:3 er** with TEMPO trapping of solvent cage escaped radicals

via

spontaneous C-N homolysis of acyl ammonium ylide

radical-radical recombination

then Nuc-H

solvent caged geminate radical pair

19